Hindawi Publishing Corporation
Advances in Mechanical Engineering
Volume 2010, Article ID 129313, 9 pages
doi:10.1155/2010/129313

Research Article

Field Synergy Principle for Energy Conservation Analysis and Application

Qun Chen,[1] Moran Wang,[2] and Zeng-Yuan Guo[1]

[1] *Key Laboratory for Thermal Science and Power Engineering of Ministry of Education, Department of Engineering Mechanics, Tsinghua University, Beijing 100084, China*
[2] *Earth and Environmental Sciences Division, Los Alamos National Laboratory, Los Alamos, NM 87545, USA*

Correspondence should be addressed to Moran Wang, mwang@lanl.gov and Zeng-Yuan Guo, demgzy@tsinghua.edu.cn

Received 28 April 2009; Accepted 5 September 2009

Academic Editor: Chen Li

Optimization of mass and energy transfer process is critical to improve energy efficiency. In this contribution we introduce the field synergy principle as a unified principle for analyzing and improving the performance of the transfer process. Three field synergy numbers are introduced for heat, mass, and momentum transfer, respectively, and three cases are demonstrated for validation. The results indicate that the field synergy numbers will increase when reducing the angle between the velocity vector and the temperature gradient or the species concentration gradient fields in the convective heat or mass transfer, and the overall heat or mass transfer capability is therefore enhanced. In fluid flows, it will reduce the fluid flow drag to decrease the synergy number between the velocity and the velocity gradient fields over the entire domain and to decrease the product between the fluid viscosity and the velocity gradient at the boundary simultaneously.

1. Introduction

Energy conservation is not only a scientific or engineering problem but also a social one that most people on this planet are facing [1–3]. Solutions of this problem include both developments of new substitutable energy products [4–6] and optimizations of current energy utilizations [7–9]. The energy efficiency is always expected maximized by enhancing the energy output for a given cost, or by minimizing the input energy loss for a given output [10]. In recent years, the multiphysical transport process in energy systems, involving mass and energy transfer, has been a hot but challenging topic [6]. The difficulties come mainly from the coupling of the multiphysical transport processes. In this work, we focus on the fluid flow coupled with species or heat transfer, which is one of the most popular transport phenomena in energy systems. In such a multiphysical process, three kinds of transports are involved: the fluid flow (momentum transport), heat transfer (energy transport), and species transfer (mass transport) [11–13].

During the past several decades, a great number of heat, mass transfer enhancement, and fluid flow drag reduction technologies have been developed including using extended surfaces, spoiler elements, and external electric or magnetic field [14–17] for heat and mass transfer, riblet surfaces, guide plates, and drag-reduction additives of low viscosity for fluid flow [18–20]. All these methods have successfully cut down not only the energy consumption but also the cost of equipment itself. In the meanwhile, in the interest of revealing the essence of these methods from the viewpoint of velocity and temperature fields, Guo et al. [21–24] proposed a concept of field synergy for enhancing convective heat transfer. They pointed out that increasing the synergy, that is, reducing the included angle, between velocity and temperature gradient, can effectively enhance convective heat transfer. Chen et al. extended this concept to the convective mass, transfer and fluid flow [25–27].

The purpose of this work is to study the transport phenomena performance based on the field synergy theory and the analogy between heat, mass and momentum transfer. The field synergy principle is available for analyzing and improving heat, mass and momentum transfer performance. Some numerical examples will be provided for validation of this principle.

2. The Analogies and the Linear Transport Laws in Transfer Processes

Momentum, heat, and mass transfer processes are always considered to be three analogous phenomena for the following two reasons: (1) the generation mechanisms are the same, that is, viscous force, thermal conduction, and mass diffusion are all caused by the motion and interaction of molecules, and (2) the govern equations of these phenomena are similar. That is, when there exists a macroscopic gradient of velocity, temperature, or concentration in an object, and the gradient is not large enough, this transport phenomenon can be described by Newton's law of viscosity, Fourier's law of heat conduction, or Fick's law of diffusion:

$$\tau_{yx} = -\mu \frac{du_x}{dy}, \tag{1}$$

$$\dot{q} = -\lambda \frac{dT}{dn}, \tag{2}$$

$$\dot{m} = -\rho D \frac{dY}{dn}. \tag{3}$$

Equation (1) describes the linear relation of the shearing force per unit area with the velocity gradient during fluid flow processes, which is the stress strain constitutive relation of Newtonian fluid. The velocity gradient is the strain, and the shearing force is the stress.

As is shown in (2) and (3), the transferred parameters are proportional to the gradients of some corresponding physical quantities, respectively, during heat and mass transfer processes, where the gradient of the temperature and the concentration are understood as "driving forces," and heat and mass crossing a unit area per unit time are the "fluxes". Furthermore, the "fluxes" have linear relationship with their corresponding "driving forces". Thus, it can be concluded that both Fourier's law and Fick's law reflect and express the general rules of diffusion processes, not the stress strain constitutive relation. It seems that neither heat nor mass transfer process is analogous to fluid flow process.

However, Newton's law of viscosity has double meanings. It expresses not only the constitutive relation of fluids but also the relationship between the velocity gradient and the momentum flux. In this connection, the velocity gradient, caused by the fluid deformation during fluid flow processes, leads to the diffusion of momentum in fluids, where the velocity gradient and the transferred momentum can therefore be thought as the driving force and the flux as momentum transport, respectively. Newton's law is the same as Fourier's law and Fick's law, which all expresses the general rules of diffusion processes. Here, (1) can also be expressed as

$$q_{mom,y} = \rho u_x v_y^* = -\mu \frac{du_x}{dy}, \tag{4}$$

where $q_{mom,y}$ stands for the momentum flux in the y direction and v_y^* is the diffusion velocity in the y direction of x-momentum component, rather than the velocity of fluid itself.

In addition, the governing equations are the energy conservation equation for convective heat transfer

$$\rho c_p \vec{U} \cdot \nabla T = \nabla \cdot (\lambda \nabla T) + Q, \tag{5}$$

the species conservation equation for convective mass transfer

$$\rho \vec{U} \cdot \nabla Y = \nabla \cdot (\rho D \nabla Y) + M, \tag{6}$$

and the momentum conservation equation for fluid flow,

$$\rho \vec{U} \cdot \nabla \vec{U} = -\nabla P + \mu \nabla^2 \vec{U} + F, \tag{7}$$

can be rewritten to a generalized form as follows:

$$\rho \vec{U} \cdot \nabla \varphi = \eta \nabla \cdot (\nabla \varphi) + G, \tag{8}$$

where $\vec{U}$ is the velocity vector, φ is the universal variable (e.g., temperature, mass fraction and velocity), η is the generalized diffusion coefficient, and G is the source term.

In summary, due to the aforementioned analogy between heat, mass, and momentum transfer, a unified principle can be developed to analyze these transfer phenomena.

3. Field Synergy Principle in Convective Heat Transfer

For two-dimensional boundary layer flows and heat transfer along a plate [23], the energy conservation equation is

$$\rho c_p \left(\vec{U} \cdot \nabla T \right) = \frac{\partial}{\partial y} \left(\lambda \frac{\partial T}{\partial y} \right). \tag{9}$$

Integrating (9) along the thermal boundary layer with the boundary condition at the outer edge of the thermal boundary layer being $(\partial T/\partial y)_{\delta_{t,x}} = 0$ gives

$$\int_0^{\delta_{t,x}} \rho c_p \left(\vec{U} \cdot \nabla T \right) dy = -\lambda \left. \frac{\partial T}{\partial y} \right|_w. \tag{10}$$

The right-hand side is the heat flux, q_w, between the solid wall and the fluid, while the left-hand side is the scalar product between the velocity vector and the temperature gradient, which can be written as

$$\int_0^{\delta_{t,x}} \rho c_p \left(\vec{U} \cdot \nabla T \right) dy = \int_0^{\delta_{t,x}} \rho c_p \left| \vec{U} \right| \left| \nabla T \right| \cos \beta_h dy, \tag{11}$$

where β_h is the included angle between the velocity vector and the temperature gradient. Thus, for two-dimensional boundary heat transfer along a plate, the boundary heat flux depends not only on the magnitude of the velocity and the temperature gradient but also on the included angle between them. It is obvious that for a fixed flow rate and temperature difference, a smaller intersection angle between the velocity and the temperature gradient will lead to a larger heat flow rate.

For a three-dimensional elliptic heat transfer process without internal heat source [28], the energy conservation equation is

$$\rho c_p \vec{U} \cdot \nabla T = \nabla \cdot (\lambda \nabla T). \tag{12}$$

Integrating this equation over the entire heat transfer domain, Ω, and transforming the volume integral to a surface integral using the Green's theorem give

$$\iiint_{\Omega} \rho c_p \vec{U} \cdot \nabla T dV = \iint_{\Gamma} \vec{n} \cdot (\lambda \nabla T) dS, \tag{13}$$

where $\vec{n}$ is the outward normal unit vector, and Γ is the boundary of the heat transfer area, which will be divided into heat transfer surfaces, adiabatic surfaces, fluid inlets, and outlets. Thus, the right-hand side of (13) is divided into four terms:

$$\begin{aligned}\iint_{\Gamma} \vec{n} \cdot (\lambda \nabla T) dS = {} & \iint_{hts} \vec{n} \cdot (\lambda \nabla T) dS + \iint_{as} \vec{n} \cdot (\lambda \nabla T) dS \\ & + \iint_{\text{in}} \vec{n} \cdot (\lambda \nabla T) dS + \iint_{\text{out}} \vec{n} \cdot (\lambda \nabla T) dS.\end{aligned} \tag{14}$$

The first term is the heat flow rate between the solid wall and the fluid. On adiabatic surfaces, the temperature gradient is zero, and so the second integral is zero. The third and fourth terms are the axial thermal diffusion at the inlet and outlet, respectively, which may be neglected when compared to the energy transferred by the fluid motion [28]. Thus, (13) is simplified as

$$\begin{aligned}&\iiint_{\Omega} \rho c_p \vec{U} \cdot \nabla T dV \\ &\quad = \iiint_{\Omega} \rho c_p \left|\vec{U}\right| |\nabla T| \cos\beta_h dV = \iint_{hts} \vec{n} \cdot (\lambda \nabla T) dS.\end{aligned} \tag{15}$$

For a convective heat transfer process, V is the volume and S_{hts} is the heat transfer surface, and then a characteristic length, $L = V/S_{hts}$, can be defined. After introducing the dimensionless variables,

$$\overline{\vec{U}} = \frac{\vec{U}}{U_{\text{in}}}, \qquad \nabla\overline{T} = \frac{\nabla T}{(T_{hts} - T_{\text{in}})/L}, \qquad d\overline{V} = \frac{dV}{V}, \tag{16}$$

equation (15) will be written in a dimensionless form as

$$Nu = \operatorname{Re}\Pr\iiint_{\Omega} \overline{\vec{U}} \cdot \nabla\overline{T} d\overline{V} = \operatorname{Re}\Pr\iiint_{\Omega} \left|\overline{\vec{U}}\right| \left|\nabla\overline{T}\right| \cos\beta_h d\overline{V}. \tag{17}$$

Equation (17) shows that the Nusselt number, that is, convective heat transfer performance, depends not only on the Reynolds number and the Prandtl number but also on the value of $\iiint_{\Omega} \overline{\vec{U}} \cdot \nabla\overline{T} d\overline{V}$.

According to the Webster Dictionary [29], when several actions or forces are cooperative or combined, such situation can be called "synergy". Thus, the above idea is named the "field synergy principle" by Guo et al. [21], and $\iiint_{\Omega} \overline{\vec{U}} \cdot \nabla\overline{T} d\overline{V}$ is named the heat transfer field synergy number, Fc_h, which represents the synergic degree of the velocity vector and the temperature gradient over the entire volume. When the heat transfer fluid is selected and the flow rate is fixed, both the Reynolds number and the Prandtl are constant, and then the heat transfer field synergy number determines the convective heat transfer capability.

For three-dimensional turbulent heat transfer without internal heat source, the time-averaged energy conservation equation is

$$\rho c_p \left\langle \vec{U} \right\rangle \cdot \langle \nabla T \rangle = \nabla \cdot [(\lambda + \lambda_t)\langle \nabla T \rangle]. \tag{18}$$

Similarly, integrating (18) over the entire heat transfer domain and transforming the volume integral to a surface integral give

$$\iiint_{\Omega} \rho c_p \left\langle \vec{U} \right\rangle \cdot \langle \nabla T \rangle dV = \iint_{hts} \vec{n} \cdot (\lambda + \lambda_t)\langle \nabla T \rangle dS, \tag{19}$$

where $\langle \vec{U} \rangle$ and $\langle \nabla T \rangle$ are the time-averaged velocity vector and the time-averaged temperature gradient, respectively. λ_t is the turbulent thermal conductivity.

The turbulent thermal conductivity vanishes at the boundary; thus (19) is simplified as

$$\iiint_{\Omega} \rho c_p \left\langle \vec{U} \right\rangle \cdot \langle \nabla T \rangle dV = \iint_{hts} \vec{n} \cdot \lambda \langle \nabla T \rangle dS. \tag{20}$$

The right-hand side is the heat flow rate between the solid wall and the fluid. Introducing some dimensionless variables, as shown in (16), to (20) gives

$$\begin{aligned}Nu &= \operatorname{Re}\Pr\iiint_{\Omega} \left\langle \overline{\vec{U}} \right\rangle \cdot \left\langle \nabla\overline{T} \right\rangle d\overline{V} \\ &= \operatorname{Re}\Pr\iiint_{\Omega} \left| \left\langle \overline{\vec{U}} \right\rangle \right| \left| \left\langle \nabla\overline{T} \right\rangle \right| \cos\beta_{ht} d\overline{V},\end{aligned} \tag{21}$$

where $\iiint_{\Omega} \langle \overline{\vec{U}} \rangle \cdot \langle \nabla\overline{T} \rangle d\overline{V}$ is the field synergy number for turbulent heat transfer, Fc_{ht}, and β_{ht} is the included angle between the time-averaged velocity vector and the time-averaged temperature gradient. For a given flow rate, increasing the field synergy number will enhance turbulent heat transfer.

The field synergy principle in convective heat transfer has been validated numerically and experimentally [21–24, 30, 31]. Based on this principle, some existing heat transfer enhancement methods will be furthermore understood. Tao et al. [22] showed that reducing the thickness of the thermal boundary layer, increasing the disturbance in the fluid, and increasing the velocity gradient at the solid wall are all unified by the field synergy principle. That is, all of these methods reduce the included angle between the (time-averaged) velocity vector and the (time-averaged)

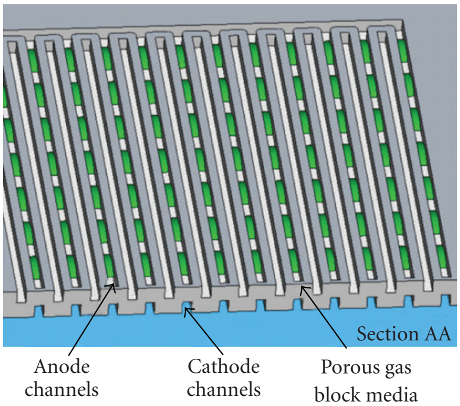

(a)

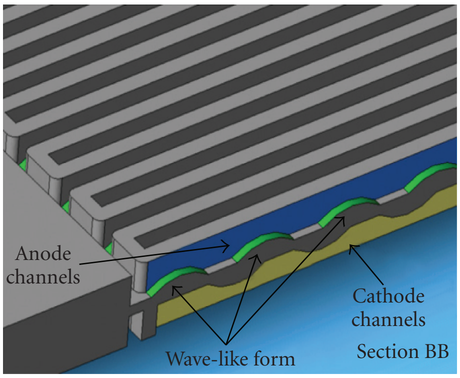

(b)

Figure 1: Cross-section and side view of gas flow channel with periodic wave-like geometry in bipolar plate of a PEMFC [35].

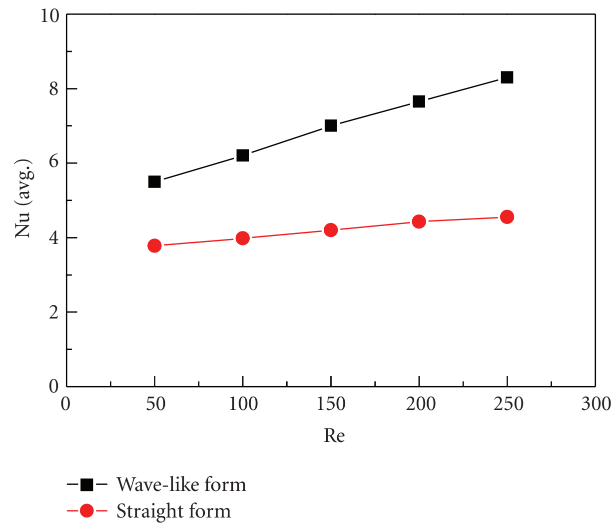

Figure 2: Variation of average Nusselt number with Reynolds number in two gas flow channel geometries (straight and wave-like) [35].

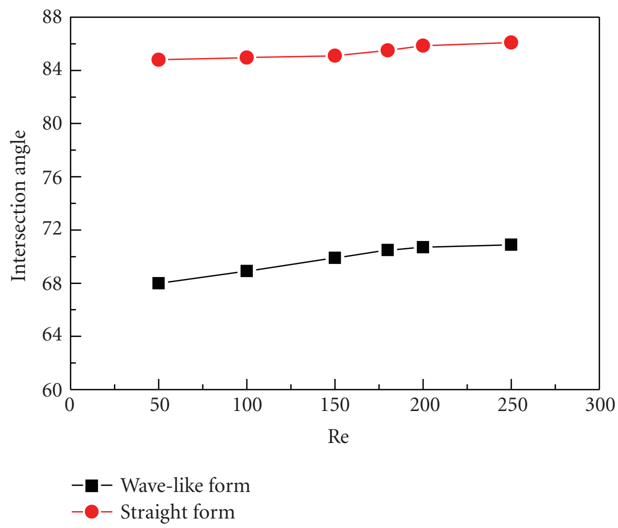

Figure 3: Variation of average intersection angle with Reynolds number in two gas flow channel geometries (straight and wave-like) [35].

temperature gradient and finally increase the field synergy number between them [31]. Moreover, the field synergy principle led to the development of some novel heat transfer enhancement technologies, such as the alternating elliptical axis tubes [32], the discrete double inclined ribs tubes [33], and the "front coarse and rear dense" slotted fins [34].

In addition, by using the field synergy principle, Kuo and Chen [35] numerically studied a gas flow channel with a periodic wave-like geometry, shown in Figure 1, to improve the heat transfer of the bipolar plate in dissipating the heat generated during the catalysis reaction and, consequently, to improve the performance of PEMFC. In this configuration, the porosity and thickness of the gas diffusion layer are 0.5 and 300 μm, respectively. The cross-section hydraulic diameter and length of the gas flow channels are 0.015 m and 0.1 m, respectively. The bipolar plate side of the channel has a wave-like form with a period of 0.01 m.

Figure 2 shows the variation of the Nusselt number with the Reynolds number in the straight and wave-like form gas flow channels, respectively. The wave-like geometry enhances the thermal performance, particularly at higher Reynolds numbers. When Re = 200, the wave-like geometry increases the value of Nu by approximately 20%. Figure 3 shows the variation of the average included angle with the Reynolds number for the straight gas flow channel and for the channel with the wave-like form geometry. When Re = 200, the average intersection angle of the velocity vector and the temperature gradient in the straight channel is 87°, while the intersection angle is reduced to 70.5° in the gas flow channel with the wave-like form geometry. Hence, improving the field synergic degree between the velocity vector and the temperature gradient by reducing their average included angleover the entire domain will improve convective heat transfer capacity.

4. Field Synergy Principle in Convective Mass Transfer

For convective mass transfer processes [25, 26], the steady-state three-dimensional species conservation equation without mass sources can be written as

$$\rho \vec{U} \cdot \nabla Y = \nabla \cdot (\rho D \nabla Y). \tag{22}$$

Integrating this equation over the entire mass transfer domain, Ω, and transforming the volume integral to the surface integral yield

$$\iiint_{\Omega} \rho \vec{U} \cdot \nabla Y dV = \iint_{\Gamma} \vec{n} \cdot (\rho D \nabla Y) dS. \tag{23}$$

Similar to convective heat transfer processes, the domain boundary will be divided into species emitting surfaces, surface without mass transfer, inlets, and outlets. Thus (23) is written as

$$\begin{aligned} &\iint_{\Gamma} \vec{n} \cdot (\rho D \nabla Y) dS \\ &= \iint_{ms} \vec{n} \cdot (\rho D \nabla Y) dS + \iint_{nms} \vec{n} \cdot (\rho D \nabla Y) dS \\ &\quad + \iint_{\text{in}} \vec{n} \cdot (\rho D \nabla Y) dS + \iint_{\text{out}} \vec{n} \cdot (\rho D \nabla Y) dS. \end{aligned} \tag{24}$$

On surfaces without mass transfer, the species concentration gradient is zero, so the second integral on the right hand is zero. At the inlet and outlet, the air velocity is high and the species concentration gradient is relatively small; and so the axial diffusion of the species at the inlet and outlet, that is, the third and fourth integrals on the right hand, can be neglected. Thus, (23) is simplified as

$$\begin{aligned} &\iiint_{\Omega} \rho \vec{U} \cdot \nabla Y dV \\ &= \iiint_{\Omega} \rho \left| \vec{U} \right| |\nabla Y| \cos \beta_m dV = \iint_{ms} \vec{n} \cdot (\rho D \nabla Y) dS, \end{aligned} \tag{25}$$

where β_m is the included angle between the velocity vector and the concentration gradient. As seen from (25), the integral of the density times the dot product of the velocity vector and the concentration gradient over the entire domains equals the overall mass flow rate, $\dot{m}$.

Introducing some dimensionless variables to (25) leads to a dimensionless form:

$$Sh = \text{Re } Sc \iiint_{\Omega} \left| \overline{\vec{U}} \right| \left| \nabla \overline{Y} \right| \cos \beta_m d\overline{V}. \tag{26}$$

Similar to turbulent heat transfer, substituting some turbulent physical parameters for laminar ones in (26) gives

$$Sh = \text{Re } Sc \iiint_{\Omega} \left| \left\langle \overline{\vec{U}} \right\rangle \right| \left| \left\langle \nabla \overline{Y} \right\rangle \right| \cos \beta_{mt} d\overline{V}, \tag{27}$$

where Sh and Sc represent the Sherwood number and the Schmidt number. $\langle \nabla \overline{Y} \rangle$ is the time-averaged species concentration gradient. Both (26) and (27) show that the Sherwood numbers for laminar and turbulent mass transfer depend not only on the Reynolds number and the Schmidt number but also on the integral value of $\overline{\vec{U}} \cdot \nabla \overline{Y}$ and $\langle \overline{\vec{U}} \rangle \cdot \langle \nabla \overline{Y} \rangle$, respectively. These values are defined as the mass transfer field synergy numbers, Fc_m or Fc_{mt}, which represent the synergy between the (time-averaged) velocity vector and the (time-averaged) species concentration over the entire volume. Similarly, when the fluid is selected, the various ways for increasing the overall strength of convective mass transfer can be classified into: (1) increasing the Reynolds number which means increasing the fluid flow rates and (2) increasing the mass transfer field synergy number. For a given fluid flow rate, the Reynolds number is constant, and the convective mass transfer capability is determined by the mass transfer field synergy number.

In the field of indoor air purification, the field synergy principle in convective mass transfer has led to the development of the decontamination ventilation designs [25] and the discrete double-inclined ribs in photocatalytic oxidation reactors [26] to enhance convective mass transfer and, consequently, to improve contaminant removal performance. To illustrate the applicability of field synergy principle for convective mass transfer processes, the decontamination quality was varied by changing the boundary conditions. The results were used to analyze the influence of the convective mass transfer field synergy on the overall mass transfer rate.

The overall mass transfer rate and field synergy number for various ventilation types are compared, including a horizontal inlet at the lower left corner (type A, Figure 4(a)), a vertical inlet at the top left corner (type B, Figure 4(b)), a horizontal inlet at the top right corner (type C, Figure 4(c)), a horizontal inlet at the top left corner (type D, Figure 4(d)), and a vertical inlet at the top right corner (type E, Figure 4(e)). The dimensions of all the rectangular cavity are: $L = 4$ mm, $H = 3$ mm, and $W_1 = W_2 = W_3 = W_4 = 0.2$ mm. The air intake velocities are 1 m/s or 2 m/s. The inlet air has a contaminant mass fraction of 0. The bottom is the contaminant source with a contaminant mass fraction of 0.01, while the left, right, and upper surfaces of the cavity all have no mass transfer.

The numerical results in Figures 5 and 6 show that for the same air inlet velocity, both the overall mass transfer rate and the mass transfer field synergy number decrease from the highest in type A to B, C, D, and the lowest in type E. For a given air inlet velocity, the Reynolds number is constant; so the overall mass transfer rate is only determined by the mass transfer field synergy number. Therefore, a better ventilation arrangement can be obtained by comparing various velocity fields for various ventilation arrangements, and by selecting the arrangement with largest mass transfer field synergy number.

5. Field Synergy Principle in Momentum Transfer-Fluid Flow

For fluid flows [27], the momentum equation for steady-state fluid flow without volume force can be written as

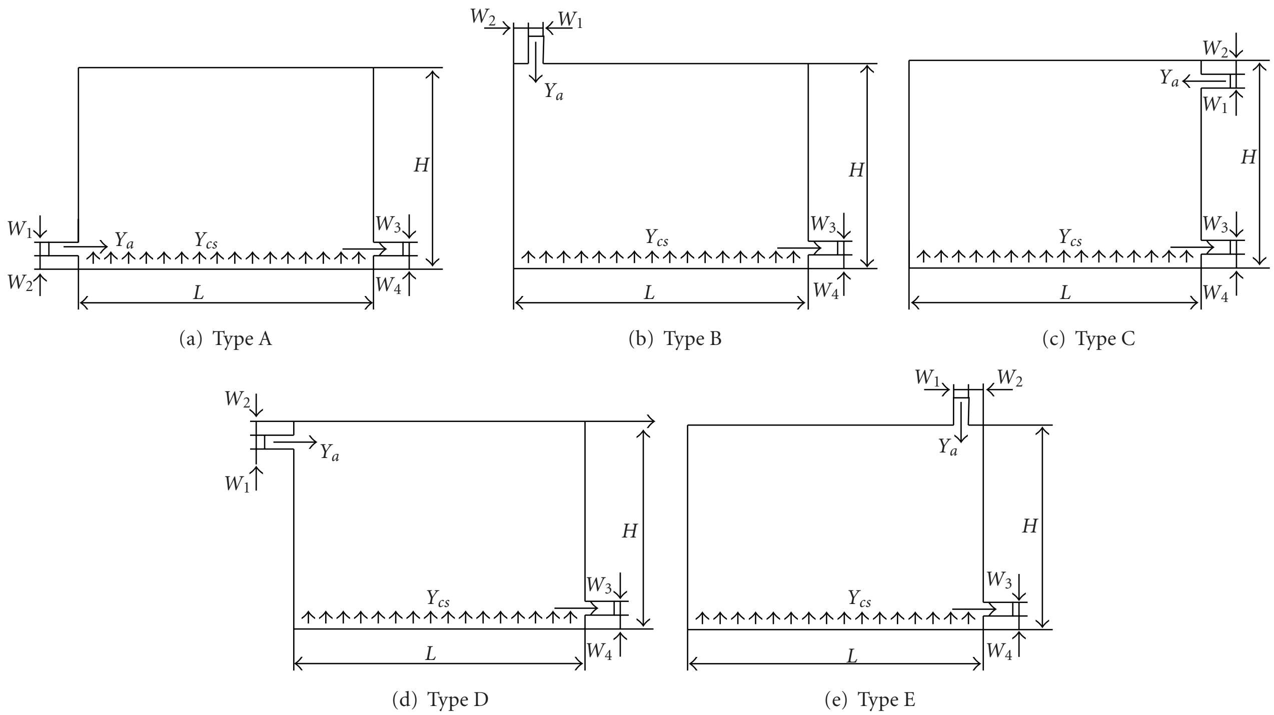

Figure 4: Sketches of ventilation configurations.

$$\rho u_j \frac{\partial u_i}{\partial x_j} = -\frac{\partial P}{\partial x_i} + \frac{\partial}{\partial x_j}\left(\mu \frac{\partial u_i}{\partial x_j}\right), \tag{28}$$

where P is the pressure, μ is the kinematic viscosity, and u_i and u_j are the velocity components in i, j direction. Integrating this equation over the entire domain, Ω, and transforming the volume integral into a surface integral, we have

$$\iiint_\Omega \rho u_j \frac{\partial u_i}{\partial x_j} dV = -\iiint_\Omega \frac{\partial P}{\partial x_i} dV + \iint_\Gamma \mu \frac{\partial u_i}{\partial x_j} \cdot \vec{n}\, dS. \tag{29}$$

By introducing the dimensionless variables

$$\overline{u}_i = \frac{u_i}{u_{\text{in}}}, \qquad \overline{u}_j = \frac{u_j}{u_{\text{in}}}, \qquad \nabla \overline{u}_i = \frac{\nabla u_i}{u_{\text{in}}/D}, \qquad d\overline{V} = \frac{dV}{V}, \qquad d\overline{S} = \frac{dS}{S}, \tag{30}$$

equation (30) can be rewritten as

$$-\frac{D}{\rho u_{\text{in}}^2} \iiint_\Omega \frac{\partial P}{\partial x_i} d\overline{V} = \iiint_\Omega \rho \overline{u}_j \frac{\partial \overline{u}_i}{\partial x_j} d\overline{V} - \frac{\mu}{\rho u_{\text{in}} D} \iint_\Gamma \nabla \overline{u}_i \cdot \vec{n}\, d\overline{S}. \tag{31}$$

The term on the left-hand side of (31) is the dimensionless pressure drop in x_i direction, denoted as the drag during the flow:

$$\Delta \overline{P}_i = -\frac{D}{\rho u_{\text{in}}^2} \iiint_\Omega \frac{\partial P}{\partial x_i} d\overline{V}. \tag{32}$$

The first term on the right-hand side is the integration of the dot product between the dimensionless velocity and the velocity gradient vectors, representing the field synergy between them in the entire domain, which referred to as the flow field synergy number:

$$\begin{aligned} FS_{\text{fi}} &= \iiint_\Omega \overline{u}_j \frac{\partial \overline{u}_i}{\partial x_j} d\overline{V} = \iiint_\Omega \overline{U} \cdot \nabla \overline{u}_i d\overline{V} \\ &= \iiint_\Omega \left|\overline{U}\right| \left|\nabla \overline{u}_i\right| \cos \beta_{fi} d\overline{V}, \end{aligned} \tag{33}$$

where β_{fi} denotes the included angle between the velocity and the x_i-velocity component gradient vectors. The value of Fc_{fi} depends not only on the velocity and the x_i-velocity component gradient but also on their included angle (their synergy). A large value of β_{fi} leads to a small value of Fc_{fi}, indicating a weak synergy between the velocity and x_i-velocity component gradient fields, and consequently a small flow drag in x_i direction. In addition, it is worth noting that the fluid viscosity μ is not involved in (34). That is, the flow field synergy number is not influenced by the fluid viscosity.

The second term on the right hand is the total dimensionless boundary viscous force due to x_i-velocity component gradient, determined by both the dynamic viscosity and the velocity gradient at the boundary:

$$\overline{\tau}_i = \frac{1}{\rho u_{\text{in}} D} \iint_\Gamma \mu \left(-\frac{\partial \overline{u}_i}{\partial x_j} \cdot \vec{n}\right) d\overline{S}. \tag{34}$$

Substituting (32), (33), and (34) into (31) gives

$$\Delta \overline{P}_i = FS_i + \overline{\tau}_i. \tag{35}$$

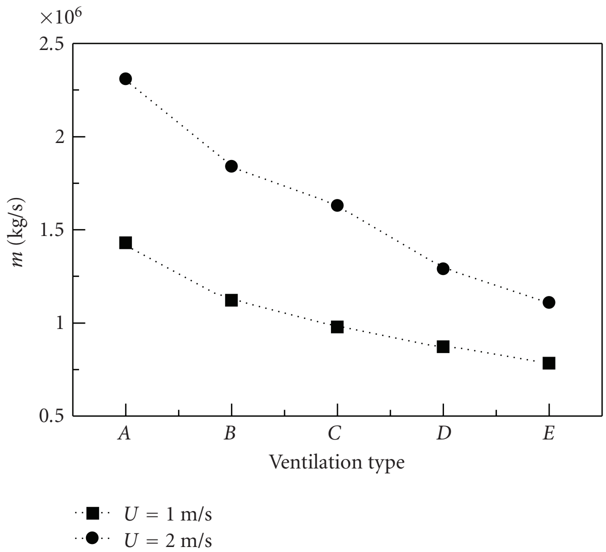

Figure 5: Decontamination rates for various ventilation arrangements.

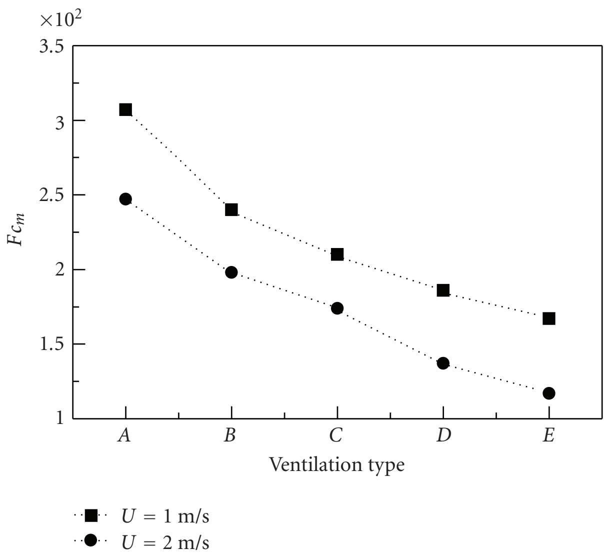

Figure 6: Field synergy numbers for various ventilation arrangements.

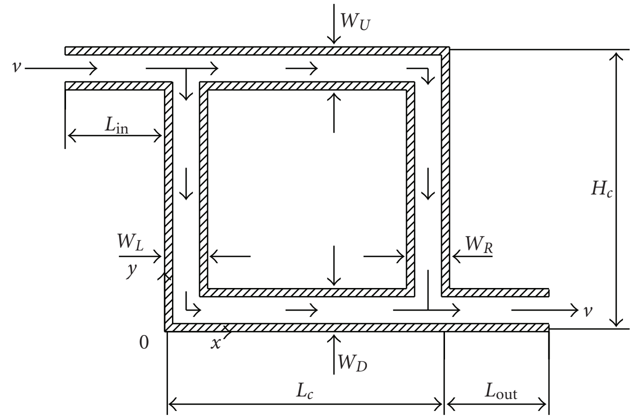

Figure 7: Sketch of the flow in a simple duct network.

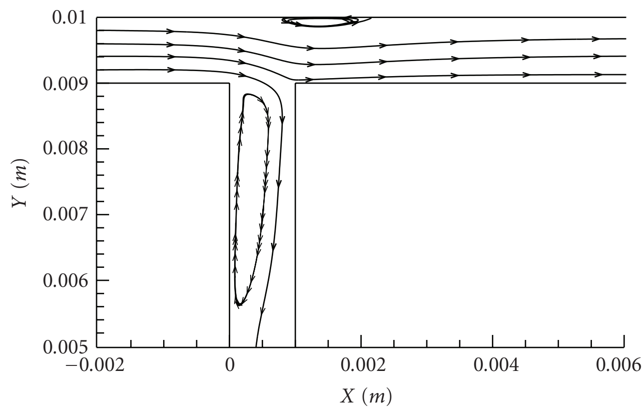

Figure 8: Air streamline field nearby the top left fork.

As is seen in (35), the flow drag depends on two factors: one is the synergy between the velocity and its gradient over the entire flow domain, and the other is the viscous force at the boundary. Hence, for a given flow rate, there are two ways to reduce the flow drag, such as (1) reducing the flow field synergy number by enlarging the synergy angle β_{fi} between the velocity and its x_i-velocity component gradient and (2) decreasing the fluid viscosity μ and/or the velocity gradient at the boundary Γ, rather than the entire flow domain. This field synergy principle in fluid flows also presents a novel approach for analyzing flow processes and sets the direction for developing new flow drag reduction technologies including designing suitable velocity distributors [27] for pipe networks and generating multilongitude vortexes during heavy oil transport processes [36].

For instance, consider a 2D fluid flow in a simple duct network [27] shown in Figure 7. The channel splits into two paths forming the shape of a rectangle which later converge back into one channel. The dimensions are $L_c = H_c = 10\,\text{mm}$, $L_{\text{in}} = L_{\text{out}} = 4\,\text{mm}$, and $W_U = W_D = W_L = W_R = 1\,\text{mm}$. The wall thickness of the duct is neglected. Air flows in the flow domain horizontally from the top left corner with a velocity of 5 m/s and out from the lower right corner. The air density and dynamic viscosity are 1.225 kg/m^3 and 1.7894 $\times 10^{-5}$ kg/(m $\cdot$ s), respectively.

Numerical results for the air streamlines nearby the top left fork are presented in Figure 8. Due to the impact of inertia, most of the air flows in the upper path straightly, while the rest is deflexed and flows in the left path. The air flow rate in the upper path is larger than the one in the left path, which increases the overall velocity gradient at the boundary. Furthermore, there exists a large clockwise vortex in the left path, which not only increases the velocity gradient at the boundary but also improves the field synergy between the velocity and its gradient. According to the field synergy principle, the above two reasons result in a large pressure

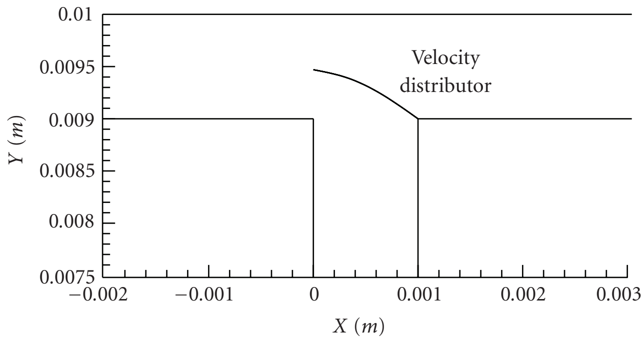

FIGURE 9: Sketch of the velocity distributor position near the top left fork.

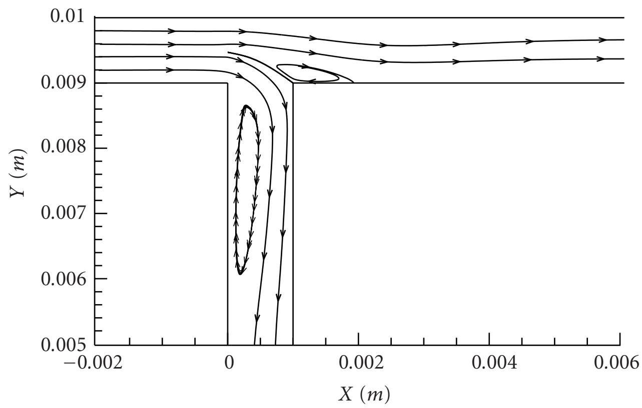

FIGURE 10: Air streamline field nearby the top left fork with a velocity distributor.

drop in the entire flow domain. In this case, the pressure drop is 47.4 Pa.

If a velocity distributor is placed along the middle streamline nearby the top left fork as shown in Figure 9, we will obtain the air streamlines as shown in Figure 10. The air flow rates in the upper and the left paths are nearly the same, which will decrease the overall velocity gradient at the boundary. In the meanwhile, compared with the result without the velocity distributor, the clockwise vortex in the left path is smaller, which reduces the field synergy number of the velocity and its gradient. As a result, the pressure drop is reduced from 47.4 to 44.9 Pa.

6. Conclusions

Due to the same generation mechanism and govern equations, momentum, heat, and mass transfer processes are the three analogous phenomena. Hence, the field synergy principle proposed earlier by Guo et al. [21] is extended from convective heat transfer to convective mass transfer and fluid flow as a unified principle for analyzing and improving the performance of these transfer phenomena.

In convective heat transfer, a smaller intersection angle, that is, a better field synergy, between the velocity and the temperature gradient will lead to a larger heat flow rate. In convective mass transfer, the overall mass transfer capability can be enhanced by decreasing the interaction angle, that is, increasing the field synergy number, between the velocity vectors and the species concentration gradients for a given fluid flow rate. In fluid flows, the flow drag depends not only on the velocity and the velocity gradient fields but also on their synergy. For a given flow rate or inlet velocity, reducing the synergy between the velocity and the velocity gradient fields over the entire domain and decreasing the fluid viscosity and the velocity gradient at the flow boundary will decrease the fluid flow drag. Several numerical examples are also provided to show the validity and applications of the principle.

Nomenclature

c_p: Specific heat capacity, J $kg^{-1}K^{-1}$
D: Mass diffusion coefficient, m^2s^{-1}
$\dot{m}$: Mass flux, kg m^{-2}
n: Gradient orientation
A: Heat transfer area, m^2
E: Entransy, J K
F: Volume force, N m^{-3}
M: Mass source, kg $s^{-1}m^{-3}$
Q: Heat source, W m^{-3}
P: Pressure, Pa
S: Surface area, m^2
$\dot{q}$: Heat flux, W m^{-2}
T: Temperature, K
$\vec{U}$: Velocity vector, m s^{-1}
V: Volume, m^3
Y: Mass friction, kg kg^{-1}
Nu: Nusselt number
Pr: Prandtl number
Re: Reynolds number
Sc: Schmidt number
Sh: Sherwood number
β: Included angel
ρ: Density, kg m^{-3}
μ: Dynamic viscosity, kg $m^{-1}s^{-1}$
η: Generalized diffusion coefficient
ϕ: Universal variable
λ: Thermal conductivity, W $m^{-1}K^{-1}$
λ_t: Turbulent thermal conductivity, W $m^{-1}K^{-1}$
$\delta_{t,x}$: Thermal boundary layer thickness, m.

Acknowledgment

This work was financially supported by the National Key Fundamental R&D Program of China (Grant no. G2007CB206901).

References

[1] N. C. Heglund, P. A. Willems, M. Penta, and G. A. Cavagna, "Energy-saving gait mechanics with head-supported loads," *Nature*, vol. 375, no. 6526, pp. 52–54, 1995.
[2] M. I. Hoffert, K. Caldeira, G. Benford, et al., "Advanced technology paths to global climate stability: energy for a

greenhouse planet," *Science*, vol. 298, no. 5595, pp. 981–987, 2002.

[3] R. K. Thauer, A.-K. Kaster, H. Seedorf, W. Buckel, and R. Hedderich, "Methanogenic archaea: ecologically relevant differences in energy conservation," *Nature Reviews Microbiology*, vol. 6, no. 8, pp. 579–591, 2008.

[4] J. Goldemberg, "Ethanol for a sustainable energy future," *Science*, vol. 315, no. 5813, pp. 808–810, 2007.

[5] D. R. Bond, D. E. Holmes, L. M. Tender, and D. R. Lovley, "Electrode-reducing microorganisms that harvest energy from marine sediments," *Science*, vol. 295, no. 5554, pp. 483–485, 2002.

[6] D. Y. Goswami, "A review and future prospects of renewable energy in the global energy system," *Advanced Technology of Electrical Engineering and Energy*, vol. 27, no. 1, pp. 55–62, 2008.

[7] B. K. Sovacool, "The importance of comprehensiveness in renewable electricity and energy-efficiency policy," *Energy Policy*, vol. 37, no. 4, pp. 1529–1541, 2009.

[8] A. M. K. P. Taylor, "Science review of internal combustion engines," *Energy Policy*, vol. 36, no. 12, pp. 4657–4667, 2008.

[9] J. Jezowski, "Review and analysis of approaches for designing optimum industrial water networks," *Chemical and Process Engineering*, vol. 29, no. 3, pp. 663–681, 2008.

[10] L. L. Lai, "A review on energy loss development," in *Proceedings of the IEEE Power and Energy Society General Meeting (PES '08)*, pp. 1–3, Pittsburgh, Pa, USA, July 2008.

[11] V. P. Carey, G. Chen, C. Grigoropoulos, M. Kaviany, and A. Majumdar, "A review of heat transfer physics," *Nanoscale and Microscale Thermophysical Engineering*, vol. 12, no. 1, pp. 1–60, 2008.

[12] Q. Chen, M. Wang, N. Pan, and Z.-Y. Guo, "Optimization principles for convective heat transfer," *Energy*, vol. 34, no. 9, pp. 1199–1206, 2009.

[13] Q. Chen, M. Wang, N. Pan, and Z.-Y. Guo, "Optimization principle for variable viscosity fluid flow and its application to heavy oil flow drag reduction," *Energy and Fuels*, vol. 23, no. 9, pp. 4470–4478, 2009.

[14] L. Yang, J. Ren, Y. Song, J. Min, and Z. Guo, "Convection heat transfer enhancement of air in a rectangular duct by application of a magnetic quadrupole field," *International Journal of Engineering Science*, vol. 42, no. 5-6, pp. 491–507, 2004.

[15] A. E. Bergles, "Heat transfer enhancement—the encouragement and accommodation of high heat fluxes," *Journal of Heat Transfer*, vol. 119, no. 1, pp. 8–19, 1997.

[16] C. F. Ma, Q. Zheng, S. C. Lee, and T. Gomi, "Impingement heat transfer and recovery effect with submerged jets of large Prandtl number liquid. I. Unconfined circular jets," *International Journal of Heat and Mass Transfer*, vol. 40, no. 6, pp. 1481–1490, 1997.

[17] L. Cheng and Y. Qiu, "The research of complex heat transfer enhancement by fluid induced vibration," *Journal of Hydrodynamics, Series B*, vol. 15, pp. 84–89, 2003.

[18] D. Neumann and A. Dinkelacker, "Drag measurements on V-grooved surfaces on a body of revolution in axial flow," *Applied Scientific Research*, vol. 48, no. 1, pp. 105–114, 1991.

[19] L. Gaudet, "Properties of riblets at supersonic speed," *Applied Scientific Research*, vol. 46, no. 3, pp. 245–254, 1989.

[20] P.-W. Li, Y. Kawaguchi, and A. Yabe, "Transitional heat transfer and turbulent characteristics of drag-reducing flow through a contracted channel," *Journal of Enhanced Heat Transfer*, vol. 8, no. 1, pp. 23–40, 2001.

[21] Z. Y. Guo, W. Q. Tao, and R. K. Shah, "The field synergy (coordination) principle and its applications in enhancing single phase convective heat transfer," *International Journal of Heat and Mass Transfer*, vol. 48, no. 9, pp. 1797–1807, 2005.

[22] W.-Q. Tao, Z.-Y. Guo, and B.-X. Wang, "Field synergy principle for enhancing convective heat transfer—its extension and numerical verifications," *International Journal of Heat and Mass Transfer*, vol. 45, no. 18, pp. 3849–3856, 2002.

[23] Z. Y. Guo, D. Y. Li, and B. X. Wang, "A novel concept for convective heat transfer enhancement," *International Journal of Heat and Mass Transfer*, vol. 41, no. 14, pp. 2221–2225, 1998.

[24] W. Q. Tao, Y. L. He, Q. W. Wang, Z. G. Qu, and F. Q. Song, "A unified analysis on enhancing single phase convective heat transfer with field synergy principle," *International Journal of Heat and Mass Transfer*, vol. 45, no. 24, pp. 4871–4879, 2002.

[25] Q. Chen, J. Ren, and Z. Guo, "Field synergy analysis and optimization of decontamination ventilation designs," *International Journal of Heat and Mass Transfer*, vol. 51, no. 3-4, pp. 873–881, 2008.

[26] Q. Chen and J. Meng, "Field synergy analysis and optimization of the convective mass transfer in photocatalytic oxidation reactors," *International Journal of Heat and Mass Transfer*, vol. 51, no. 11-12, pp. 2863–2870, 2008.

[27] Q. Chen, J. Ren, and Z. Guo, "Fluid flow field synergy principle and its application to drag reduction," *Chinese Science Bulletin*, vol. 53, no. 11, pp. 1768–1772, 2008.

[28] W. M. Kay and M. E. Craw, *Convective Heat and Mass Transfer*, McGraw-Hill, New York, NY, USA, 1980.

[29] D. B. Guralnik, Ed., *WEBSTER'S New World Dictionary of the American Language*, William Collins, Cleveland, Ohio, USA, 2nd edition, 1979.

[30] M. Zeng and W.-Q. Tao, "Numerical verification of the field synergy principle for turbulent flow," in *Proceedings of the International Conference on Energy Saving and Enhancement of Heat Transfer*, Guangzhou, China, October 2004.

[31] Y. L. He, W. Q. Tao, F. Q. Song, and W. Zhang, "Three-dimensional numerical study of heat transfer characteristics of plain plate fin-and-tube heat exchangers from view point of field synergy principle," *International Journal of Heat and Fluid Flow*, vol. 26, no. 3, pp. 459–473, 2005.

[32] J.-A. Meng, X.-G. Liang, Z.-J. Chen, and Z.-X. Li, "Experimental study on convective heat transfer in alternating elliptical axis tubes," *Experimental Thermal and Fluid Science*, vol. 29, no. 4, pp. 457–465, 2005.

[33] X. Li, J. Meng, and Z. Guo, "Turbulent flow and heat transfer in discrete double inclined ribs tube," *International Journal of Heat and Mass Transfer*, vol. 52, no. 3-4, pp. 962–970, 2009.

[34] Y. P. Cheng, Z. G. Qu, W. Q. Tao, and Y. L. He, "Numerical design of efficient slotted fin surface based on the field synergy principle," *Numerical Heat Transfer, Part A*, vol. 45, no. 6, pp. 517–538, 2004.

[35] J.-K. Kuo and C.-K. Chen, "Evaluating the enhanced performance of a novel wave-like form gas flow channel in the PEMFC using the field synergy principle," *Journal of Power Sources*, vol. 162, no. 2, pp. 1122–1129, 2006.

[36] Q. Chen, *Irreversibility and Optimization of Convective Transport Processes*, Tsinghua University, Beijing, China, 2008.